JOURNAL OF SOLID STATE CHEMISTRY 66, 171–180 (1987)

Synthesis and Crystal Structures of the Manganous Antimonates $Mn_2Sb_2O_7$ and $MnSb_2O_6$

H. G. SCOTT

CSIRO, Division of Materials Science, Locked Bag 33, Clayton, Victoria, Australia 3168

Received February 18, 1986; in revised form April 28, 1986

$Mn_2Sb_2O_7$ has been prepared by the solid state reaction of $MnCO_3$ and Sb_2O_3 at 1100°C, and its crystal structure determined from X-ray powder diffraction data. The compound is trigonal $P3_121$ with a = 7.191, c = 17.398 Å, and the structure is fluorite-related, but not a distorted pyrochlore. The relationship between this structure and that of pyrochlore is discussed. $MnSb_2O_6$ was formed as a reaction intermediate and its structure has also been determined. This phase is trigonal $P321$ with a structure related to that of Na_2SiF_6 and is apparently a new polymorph, since $MnSb_2O_6$ has previously been stated to have either the orthorhombic columbite or the tetragonal trirutile structure. © 1987 Academic Press, Inc.

Introduction

In 1963 Aia *et al.* (*1*) reported the preparation of a cubic manganese fluoantimonate which they considered to have the pyrochlore structure. However they did not determine the crystal structure or even the composition of the compound. Subsequently, Brisse *et al.* (*2*) prepared $Mn_2Sb_2O_7$ by Baccaredda's method (*3*) and also by the reaction of MnO_2 and Sb_2O_3. The compound was stable in air only below 600°C; its X-ray powder diffraction pattern was not well defined but was consistent with that of a pyrochlore structure. Oxide pyrochlores may be typified by $Hg_2Nb_2O_7$ (*4*) which is cubic, space group $Fd3m$, with a lattice parameter of 10.453 Å. The structure has Nb at 16*c* (0,0,0) sites, Hg at 16*d* (1/2, 1/2, 1/2) sites, and O at 8*b* (3/8, 3/8, 3/8) and 48*f* (0.323, 1/8, 1/8) sites.

Recently, Subramanian *et al.* (*5*) prepared $Mn_2Sb_2O_7$ by firing the mixed oxides in a sealed platinum tube at 1100°C. This material gave a sharp X-ray powder diffraction pattern, and on the basis of that pattern, together with magnetic and Mossbauer data, was described as having a rhombohedrally distorted pyrochlore structure. However, while the *d* spacings in the diffraction pattern are generally consistent with a rhombohedral distortion of pyrochlore, the intensities of the reflexions do not support that description of the structure. If the $Mn_2Sb_2O_7$ structure were a slight distortion of the pyrochlore type, the intensities of the reflexions would be directly related by multiplicity factors to the intensities of the corresponding pyrochlore reflexions. This is not the case (see Appendix).

As Brisse *et al.* (*2*) and also Subramanian *et al.* (*6*) point out, the stability field of the 2 : 5 oxide pyrochlores is not well defined, as the literature contains few unambiguous

0022-4596/87 $3.00
Copyright © 1987 by Academic Press, Inc.
All rights of reproduction in any form reserved.

examples of the type. Consequently, new 2:5 pyrochlores would help to define this field, and claims of such compounds need to be scrutinized carefully.

Some compounds originally described as rhombohedral pyrochlores, $Pb_2Nb_2O_7$ and $Pb_2Ta_2O_7$ for example (*7–10*), have subsequently been shown to have more complex pyrochlore-related structures, and may not even have the ideal composition (*11–13*). It was therefore decided to reexamine $Mn_2Sb_2O_7$ to establish the true composition or composition range, and to determine whether a different fluorite-related structure might better explain the observed X-ray powder diffraction pattern.

In the course of the work, another phase was found to form as a precursor to $Mn_2Sb_2O_7$. This phase was shown to have the composition $MnSb_2O_6$, and a trigonal structure related to, but distinct from, that of NiU_2O_6 (*14*) and Lu_2TeO_6 (*15*), both of which have the Na_2SiF_6 structure (*16*). The crystal structure of this phase has been successfully determined from X-ray powder diffraction data.

Experimental Methods

The preparative techniques essentially followed those of Subramanian *et al.* (*5*). The starting materials were laboratory reagent grade Sb_2O_3 (>99%) and $MnCO_3$. The latter was precipitated from $MnSO_4$ solution by the addition of $NaHCO_3$ solution: analytical grade reagents were used, and since the product could not be completely dried without risk of decomposition it was assayed by ignition to Mn_2O_3 at 600°C.

The required quantities of the starting materials were milled together in a boron carbide mortar under 1:1:1 trichloroethane, allowed to dry, and pressed into pellets which were fired in air on platinum foil in an electric furnace. The samples were weighed at intervals during the firing cycle to provide information on the reactions occurring and to check on possible loss by evaporation.

The phases present in the fired samples were identified by powder X-ray diffraction, using a Guinier camera with Cu$K\alpha_1$ radiation. To reduce the effect of manganese fluorescence a thin copper or aluminium screen was placed in front of the film. When accurate lattice parameters were required, thoria (a = 5.5972 Å) was included as an internal standard. X-Ray intensity data were obtained by planimetry of microdensitometer scans of the Guinier photographs. Series of two or more films with different exposures were used to provide reliable measurements of both strong and weak reflexions.

Results

Compound Formation

(*i*) *Pyrochlore composition.* A mixture of the reactants calculated to yield the ideal pyrochlore composition was fired at successively higher temperatures from 450 to 1250°C. After each firing a small portion of the sample was removed for X-ray diffraction analysis to determine the phases present. Details of the firing conditions and products are given in Table I.

Below 600°C there was no perceptible reaction between the components, which had however been converted to Mn_2O_3 and α-Sb_2O_4. At 900°C the first compound to form was a trigonal phase subsequently shown to be a polymorph of $MnSb_2O_6$. At 950°C some $Mn_2Sb_2O_7$ formed, and the reaction was complete after 72 hr at 1100°C. At all these temperatures the sample mass was consistent with the products indicated in Table I.

At 1200°C and above appreciable mass loss occurred, presumably by evaporation of Sb as one of its oxides, but even after a 10% mass loss the powder diffraction pattern contained only one weak line which could not be ascribed to the $Mn_2Sb_2O_7$

TABLE I

PRODUCTS OF THE SOLID STATE REACTION $2MnCO_3 + Sb_2O_3$

Temperature (°C)	Reaction time (hr)	Reaction products	Comments
600	24	Mn_2O_3 + α-Sb_2O_4	
900	24	Mn_2O_3 + γ-$MnSb_2O_6$	
950	24	Mn_2O_3 + $Mn_2Sb_2O_7$ + γ-$MnSb_2O_6$	
950	96	$Mn_2Sb_2O_7$ + γ-$MnSb_2O_6$ + ?	Trace of unidentified phase
1100	72	$Mn_2Sb_2O_7$	
1200	24	$Mn_2Sb_2O_7$	2.7% mass loss
1250	24	$Mn_2Sb_2O_7$ + ?	7.3% mass loss

phase. This weak line at d = 4.99 Å could not reasonably be explained by any known compound in the Mn–Sb–O system.

(*ii*) *Range of homogeneity.* To investigate a possible composition range for the $Mn_2Sb_2O_7$ phase, compositions on either side of stoichiometry were prepared and examined. Table II sets out the compositions used, the firing conditions, the phases found, and their lattice parameters. The variations in the lattice parameters of the $Mn_2Sb_2O_7$ phase, depending on whether it coexists with Mn_3O_4 or $MnSb_2O_6$, are apparently statistically significant and suggest a narrow range of homogeneity.

(*iii*) *Other compounds.* To confirm that the major phase found at the 2MnO + Sb_2O_3 composition after firing at 900°C was $MnSb_2O_6$, reactants corresponding to this latter composition were mixed and fired at 1100°C. A single phase was formed which, apart from improved crystallinity due to the higher firing temperature, was identical to the trigonal phase formed at 900°C in the 2MnO + Sb_2O_3 mixture. It has been designated γ-$MnSb_2O_6$ to distinguish it from previously reported columbite (*17*) and trirutile (*18*) polymorphs with this composition.

Crystal Structures

Crystal structures were refined using the program POWDER (*19*). Scattering factors for neutral atoms were used (*20*) without correction for anomalous dispersion. The weighting scheme used was $W(I) = 10.0/(1.0 + I)$, corresponding to standard deviations for the measured intensities ranging

TABLE II

LATTICE PARAMETERS OF $Mn_2Sb_2O_7$ PHASE IN SAMPLES OF DIFFERENT OVERALL COMPOSITION, AFTER FIRING FOR 72 HR AT 1100°C

Nominal composition	Phases present	Lattice parameters (Å)	
		a	*c*
$14MnO + 5Sb_2O_5$	Mn_3O_4 + $Mn_2Sb_2O_7$	7.1885(2)	17.3986(7)
$2MnO + Sb_2O_5$	$Mn_2Sb_2O_7$	7.1903(18)	17.3951(11)
$10MnO + 7Sb_2O_5$	$Mn_2Sb_2O_7$ + γ-$MnSb_2O_6$	7.1933(8)	17.3974(24)

Note. Figures in parentheses, here and elsewhere, are estimated standard deviations in the last quoted decimal place.

from about 3 for the strongest reflexion for which $I = 100$, to about 0.3 for unobserved reflexions. These errors are reasonable for Guinier camera intensity data. The weighted residual, Rw, is $\frac{1}{2}[\Sigma w\Delta I^2/\Sigma wI^2]^{1/2}$.

(*i*) $Mn_2Sb_2O_7$. Diffraction data were collected to a maximum diffraction angle of $2\theta = 60°$. On the basis of the lattice parameters and the d spacings of the stronger reflexions, it was concluded that the structure was fluorite-related with trigonal symmetry. Different cation arrangements consistent with this model were investigated as trial structures using a truncated data set including only reflexions with $2\theta < 30°$, since these reflexions are the most sensitive to the cation ordering.

When scale and an overall temperature factor were refined, the pyrochlore arrangement of cations yielded $R_w = 35\%$, and there was no apparent correlation between the observed and calculated intensities of the low-angle reflexions. In contrast, another cation arrangement yielded $R_w = 16.5\%$ and gave a good qualitative description of the observed intensities.

The preferred model has a cation arrangement which can be described in $P3_121$. The structure was refined in this space group using the full data set and, after some problems with degeneracy had been overcome, yielded $R_w = 5.5\%$. The refined parameters for this structure are given in Table III and derived bond lengths are shown in Table IV. Observed and calculated intensities and measured d spacings are given in Table V.

A variant of this structure, in which Mn and Sb atoms were interchanged, was also satisfactory at the stage where cation ordering alone was considered. However, this model did not refine well, and it also had an

TABLE III

CRYSTAL STRUCTURE DATA FOR $Mn_2Sb_2O_7$

Trigonal $P3_121$ $Z = 6$
$a = 7.191(1)$ Å $c = 17.398(1)$ Å

Atom	Site	Atomic coordinates		
		x	y	z
Mn1	3(*a*)	0.82(2)	0	$\frac{1}{3}$
Mn2	3(*b*)	0.83(2)	0	$\frac{5}{6}$
Mn3	6(*c*)	0.68(2)	0.20(2)	−0.005(4)
Sb1	3(*a*)	0.32(1)	0	$\frac{1}{3}$
Sb2	3(*b*)	0.33(1)	0	$\frac{5}{6}$
Sb3	6(*c*)	0.50(1)	0.34(1)	0.165(2)
O1	6(*c*)	0.19(4)	0.20(3)	0.146(10)
O2	6(*c*)	0.68(4)	0.62(3)	0.188(9)
O3	6(*c*)	0.20(3)	0.55(3)	0.126(11)
O4	6(*c*)	0.01(6)	0.32(5)	0.064(8)
O5	6(*c*)	−0.04(4)	0.84(5)	0.040(8)
O6	6(*c*)	0.52(6)	0.40(3)	0.061(11)
O7	6(*c*)	0.50(7)	0.80(6)	0.055(9)

Note. B(Mn) = 1.1(8) Å², B(Sb) = 1.4(4) Å², B(O) = −0.4(17) Å². $R_w = 5.50\%$. $\chi^2/\nu = 1.193$ (74 observations, 35 parameters).

TABLE IV

CALCULATED BOND LENGTHS IN $Mn_2Sb_2O_7$, BASED ON PARAMETERS IN TABLE III

Bond	Length (Å)	Bond	Length (Å)
Mn1–O1	2.55	Sb1–O2	3.31[a]
–O4	2.23	–O5	1.90
–O5	2.27	–O6	2.05
–O6	2.39	–O7	2.09
Mn2–O1	2.34	Sb2–O1	2.03
–O2	2.04	–O3	1.67[b]
–O3	3.09[b]	–O4	1.78
–O5	2.23		
Mn3–O3	2.34	Sb3–O1	1.98
–O4	2.41	–O2	1.81
–O4′	2.46	–O2′	2.55
–O5	2.40	–O3	2.22
–O6	2.66	–O6	1.86
–O7	2.55	–O7	1.99
–O7′	2.24		

Note. E.s.d.'s in the bond lengths are determined primarily by those of the oxygen coordinates, which range from 0.28 Å in the xy plane to 0.16 Å in the z direction.

[a] Sb1 is formally 8-coordinated by oxygen, but O2 is clearly not part of the actual coordination.

[b] These unacceptable bond lengths are both associated with O3.

TABLE V

X-RAY POWDER DIFFRACTION DATA FOR $Mn_2Sb_2O_7$

h k l	d_{meas}	I_{obs}	I_{calcd}	*h k l*	d_{meas}	I_{obs}	I_{calcd}
1 0 0	6.22	1.6	1.5	3 0 4	1.8741	d.m.	0.5
1 0 1	5.86	5.2	5.1	1 1 8	1.8605	d.m.	0.5
0 0 3	5.80	8.2	8.6	1 0 9	—	n.o.	0.3
1 0 2	5.06	11.5	10.7	2 1 6	—	n.m.	0.3
1 0 3	4.243	3.9	3.8	2 2 0	1.7970	32.0	32.3
1 1 0	3.594	4.1	4.1	2 2 1	—	n.o.	0.2
1 0 4	3.566	6.7	6.3	3 0 5	1.7832	29.3	27.5
1 1 1	3.521	2.0	1.9	2 0 8			
1 1 2	3.323	2.6	2.8	2 2 2	—	n.o.	0.2
2 0 0	—	n.o.	0.1	3 1 0	—	n.m.	0.2
2 0 1	3.065	10.7	9.2	3 1 1	—	n.o.	0.4
1 1 3	—	n.o.	0.3	2 2 3	1.7167	3.1	1.1
1 0 5	3.038	1.5	1.6	2 1 7	1.7082	d.m.	0.8
2 0 2	2.931	100.0	101.5	1 1 9	1.7018	d.m.	0.1
0 0 6	2.899	32.8	32.8	3 1 2	1.6938	d.m.	1.2
1 1 4	—	n.m.	0.6	3 0 6	1.6868	d.m.	0.7
2 0 3	—	n.o.	0.1	1 0 10	1.6754	d.m.	1.0
1 0 6	—	n.o.	0.1	2 2 4	—	n.o.	0.1
2 0 4	2.530	39.9	41.5	3 1 3	1.6548	d.m.	0.2
1 1 5	—	n.m.	0.6	2 0 9	—	n.o.	0.1
2 1 0	—	n.m.	0.1	3 1 4	1.6052	d.m.	0.6
2 1 1	2.332	d.m.	0.8	2 2 5	1.5964	d.m.	0.4
2 0 5	—	n.o.	0.4	2 1 8			
1 0 7	—	n.o.	0.3	3 0 7	—	n.o.	0.3
2 1 2	2.271	0.8	0.8	1 1 10	—	n.m.	0.2
1 1 6	2.257	1.4	1.3	4 0 0	—	n.o.	0.1
2 1 3	—	n.o.	0.1	4 0 1	1.5501	2.2	1.5
2 0 6	—	n.o.	0.1	4 0 2	1.5317	14.6	13.5
3 0 0	—	n.m.	0.6	2 2 6	1.5275	24.8	24.4
2 1 4	2.070	3.1	2.5	2 0 10	1.5182	15.7	15.1
3 0 1	2.060	d.m.	0.9	4 0 4	1.4654	9.9	8.4
1 0 8	—	n.o.	0.0	0 0 12	1.4494	3.3	2.7
1 1 7	—	n.o.	0.3	4 0 8	1.2654	7.1	7.2
3 0 2	2.017	1.0	0.5	4 2 2	1.1658	8.0	8.8
3 0 3	—	0.6	0.3	4 0 10	1.1603	4.3	4.6
2 1 5	—	0.9	0.9	2 0 14	1.1541	3.8	3.6
2 0 7	—	1.2	1.1	2 4 4	1.1357	5.4	6.0
0 0 9	1.9327	1.9	1.3	2 2 12	1.1286	7.0	7.0

Note. Reflexions with intensities too weak to measure were classified as not observed (n.o.), not measurable (n.m.), or *d*-spacing measured (d.m.) and assigned intensities of 0.0, 0.25, or 0.50, respectively. Non-equivalent *h k l* and *k h l* reflexions are not listed separately.

implausible arrangement for the formal anion vacancies. It was therefore rejected.

Some comments on the parameters in Table III are necessary. The temperature factor for oxygen relative to those of the cations is unsatisfactory, but in view of its very large standard deviation it is not unacceptable. In any case temperature factors obtained from Guinier data are of doubtful physical significance because of correla-

tions with specimen absorption (*21*). The precision of the parameter estimates, in particular those for the anion coordinates, is very low, but this is an inevitable consequence of a low ratio of observations to parameters varied of about 2 : 1.

(*ii*) $MnSb_2O_6$. Diffraction data were collected to a maximum 2θ of 87°. The lattice parameters and *d* spacings of the strongest reflexions suggested that the structure might be isomorphous with that of the tellurates Ln_2TeO_6, Sc_2TeO_6, and In_2TeO_6 (*15*, *22*) and uranates CoU_2O_6 and NiU_2O_6 (14) which have the Na_2SiF_6 structure (*16*). The density of the phase, measured pycnometrically, was 5.88 Mg m^{-3}, compared with an X-ray density of 6.19 Mg m^{-3} for the Na_2SiF_6-type structure.

The initial trial structure based on the Na_2SiF_6 type was not successful. R_w was 32%, for a truncated data set with $2\theta < 65°$, and apart from the strongest reflexions there was little correlation between observed and calculated intensities.

TABLE VI

CRYSTAL STRUCTURE DATA FOR γ-$MnSb_2O_6$

Trigonal *P*321 $Z = 3$
$a = 8.8054(4)$ Å $c = 4.7229(4)$ Å
$D_m = 5.88$ Mg m^{-3} $D_x = 6.193$ Mg m^{-3}
$V = 317.13$ Å^3

Atom	Site	Atomic coordinates[a]		
		x	*y*	*z*
Sb1	1(*a*)	0	0	0
Sb2	2(*d*)	⅓	⅔	0.509(9)
Sb3	3(*f*)	0.305(1)	0	½
Mn	3(*e*)	0.632(2)	0	0
O1	6(*g*)	0.095(11)	−0.115(6)	0.766(8)
O2	6(*g*)	0.474(12)	−0.408(10)	0.744(10)
O3	6(*g*)	0.229(9)	−0.232(12)	0.279(10)

Note. B(Mn) = 1.42(43) Å^2, B(Sb) = 1.45(15) Å^2, B(O) = 1.15(63) Å^2. $R_w = 4.22\%$. $\chi^2/\nu = 0.978$ (62 observations, 16 parameters).

[a] Asymmetric unit chosen to correspond with that adopted by Kemmler-Sack for NiU_2O_6 (*14*).

TABLE VII

CALCULATED BOND LENGTHS[a] IN γ-$MnSb_2O_6$, BASED ON PARAMETERS IN TABLE VI

Bond	Length (Å)	Mean values (Å)	
Sb1–O1	1.95	1.95	
Sb2–O2	2.00		
Sb2–O3	1.91	1.96	1.99
Sb3–O1	2.04		
Sb3–O2	2.05	2.06	
Sb3–O3	2.08		
Mn–O1	2.24		
Mn–O2	2.09	2.18	
Mn–O3	2.20		

Note. e.s.d.'s for the bond lengths are about 0.07 Å.

[a] Bond lengths in this table and in Table IV are calculated from the refined parameters before rounding to the values in Tables VI and III, respectively.

An alternative noncentrosymmetric model with a different arrangement of cations on the same set of cation sites was more promising. R_w was 21.3%, and the qualitative fit of intensities was fair. When this model was refined with the full data set, R_w fell to 4.22%. The parameter changes on the final cycle were all less than one-tenth of their respective standard deviations. The refined parameters and derived bond lengths are given in Tables VI and VII, respectively. Observed and calculated intensities and measured *d* spacings are shown in Table VIII.

Discussion

The existence of the compound $Mn_2Sb_2O_7$ reported by Subramanian *et al.* (*5*) has been confirmed. Precision lattice parameter measurements suggest that the phase may have a narrow range of composition since there are small but significant differences between the parameters measured for samples prepared on either side of stoichiometry, depending on whether $Mn_2Sb_2O_7$ coexists with Mn_3O_4 or $MnSb_2O_6$.

The X-ray powder diffraction pattern ob-

TABLE VIII

X-RAY POWDER DIFFRACTION DATA FOR γ-$MnSb_2O_6$

$h\ k\ l$	d_{meas}	I_{obs}	I_{calcd}	$h\ k\ l$	d_{meas}	I_{obs}	I_{calcd}
1 0 0	—	n.m.	0.8	3 3 0	1.4676	22.3	19.8
0 0 1	4.722	23.8	23.9	2 0 3	1.4550	6.0	5.4
1 1 0	4.402	27.6	26.7	5 0 1	1.4513	10.9	9.7
1 0 1	4.015	32.4	34.7	4 2 0	1.4410	4.5	4.0
2 0 0	—	n.o.	0.1	3 2 2	—	n.m.	1.3
1 1 1	3.220	100.0	100.9	3 3 1	—	4.4	3.5
2 0 1	2.968	47.9	51.5	2 1 3	1.3819	8.2	7.3
2 1 0	2.882	5.0	5.2	4 2 1	1.3785	4.6	4.0
3 0 0	2.542	63.4	61.7	5 1 0	1.3695	2.8	2.6
2 1 1	2.461	32.7	33.4	4 1 2	1.3605	4.6	3.9
0 0 2	2.362	14.2	12.5	3 0 3	1.3384	4.2	4.7
1 0 2	—	n.o.	0.1	5 1 1	1.3155	11.1	9.8
3 0 1	2.239	27.7	25.6	5 0 2	1.2806	5.0	4.7
2 2 0	2.202	2.4	2.1	2 2 3			
3 1 0	2.116	2.6	2.7	6 0 0	1.2712	4.9	5.2
1 1 2	2.082	4.3	4.6	3 1 3	—	n.o.	0.8
2 0 2	—	n.o.	0.3	4 3 0	—	n.o.	1.2
2 2 1	1.9953	19.2	18.7	3 3 2	1.2465	7.8	8.3
3 1 1	1.9308	3.6	3.0	4 2 2		1.9	2.2
4 0 0	—	n.o.	0.8	6 0 1		1.7	2.7
2 1 2	1.8271	5.2	5.9	5 2 0		2.0	2.0
4 0 1	—	n.o.	0.1	4 0 3		n.o.	0.1
3 2 0	1.7493	2.8	2.6	4 3 1		n.o.	0.1
3 0 2	1.7303	69.8	70.7	5 1 2			
4 1 0	1.6639	3.6	3.5	5 2 1		(18.7)	12.1
3 2 1	1.6398	26.2	24.9	0 0 4			
2 2 2	1.6099	3.9	3.8	3 2 3		6.9	8.2
3 1 2	—	3.3	3.4	1 0 4		n.o.	0.2
0 0 3				6 1 0		n.o.	0.6
4 1 1	1.5694	14.3	13.9	4 1 3		4.6	5.3
1 0 3	—	n.m.	1.3	1 1 4		n.o.	1.1
5 0 0	—	n.o.	0.0	6 1 1		n.o.	0.3
4 0 2	1.4825	9.0	9.5	2 0 4		n.o.	0.0
1 1 3				6 0 2		10.3	12.1

Note. Reflexions with intensities too weak to measure were classified as not observed (n.o.) or not measurable (n.m.) and assigned intensities of 0.3 or 1.0 respectively. Nonequivalent $h\ k\ l$ and $k\ h\ l$ reflexions are not listed separately. I_{obs} in parentheses is not included in refinement.

tained from the phase agrees well with that described by Subramanian *et al.* (5), though numerous additional weak reflexions were observed and indexed. These weak reflexions include some for which $-h + k + l \neq 3n$, so that the symmetry is trigonal or hexagonal, rather than rhombohedral as previously proposed. All the strong reflexions can be indexed on the basis of a trigonally distorted fluorite-type subcell, so that it is reasonable to assume that the structure of $Mn_2Sb_2O_7$ is fluorite-related, with the supercell, i.e., the true unit cell, determined by the cation arrangement on sites permitted by the subcell–supercell relationship. The cation arrangement corresponding to

pyrochlore ordering does not give a satisfactory explanation of the X-ray reflexion intensities. However, an alternate fluorite-related structure does explain these intensities and has been refined successfully in the space group $P3_121$.

The proposed structure cannot be regarded as definitive. The ratio of observations to parameters varied is low, and the nonequivalent *hkl* and *khl* reflexions cannot be resolved with powder data, so that precision is poor. Nevertheless, the structure provides an acceptable description of the reflexion intensities, indicated by a goodness-of-fit index close to unity. Also, the average bond lengths and coordination numbers are consistent with generally accepted values. The bond lengths shown in Table IV exhibit considerable variation. Nevertheless, the overall mean values of 2.41 Å for Mn^{2+}–O^{2-} and 1.97 Å for Sb^{5+}–O^{2-} are in vary fair agreement with the expected values of 2.34 and 1.98 Å, respectively, derived from Shannon's compilation of ionic radii (*23*). Two exceptional bond lengths in Table IV, and an unacceptable oxygen–oxygen distance of 1.87 Å, are all associated with the same oxygen atom. Finally, the structure provides a natural explanation for the trigonal distortion of the subcell relative to the ideal cubic form: this distortion is not so easily explained if cubic pyrochlore cation ordering is assumed.

The relationship between the structure proposed here for $Mn_2Sb_2O_7$ and the pyrochlore type is most easily understood in terms of the description given by Darriet *et al.* (*24*) and Yagi and Roth (*25*). In this view, the pyrochlore structure is composed of an alternation parallel to (111) of "hexagonal tungsten bronze" (HTB) layers of corner-linked BO_6 octahedra and "isolated octahedron" (IO) layers. The stacking of the layers is such that all octahedra share all their corners with adjacent octahedra, giving rise to a rigid 3-dimensional framework.

In the $Mn_2Sb_2O_7$ structure the same alternation of HTB and IO layers occurs, but the stacking is different and the isolated octahedra share only four of their six corners. It is postulated that this results in a less rigid framework able to accommodate divalent cations which could not form a true pyrochlore. The different stacking sequences are illustrated in Fig. 1.

The review by Subramanian *et al.* (6) only reports structure determinations for A_2^{2+} B_2^{5+} O_7^{2-} pyrochlores in which A is Cd or Hg, with ionic radii in 8-fold coordination of 1.10 and 1.14 Å, respectively. Consequently it is not surprising that Mn^{2+}, with radius 0.96 Å, does not form a pyrochlore with Sb^{5+}.

During the preparation of $Mn_2Sb_2O_7$, a precursor phase formed that also has trigonal symmetry. The composition of the phase was shown to be $MnSb_2O_6$, and it has been designated γ-$MnSb_2O_6$ to distinguish it form the previously reported orthorhombic columbite (*17*) and tetragonal

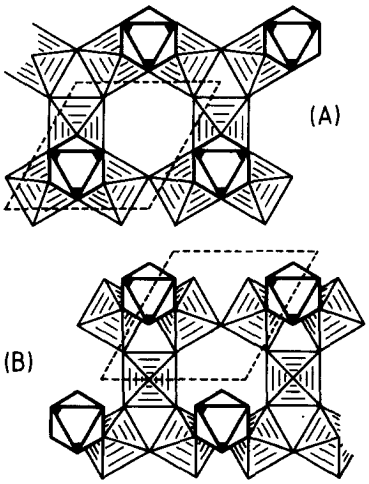

FIG. 1. Idealized view down [111] fluorite subcell direction of corner-linked BO_6 octahedra, showing the different stackings of the "hexagonal tungsten bronze" layer (light lines) and "isolated octahedron" layer (heavy lines) in the (A) pyrochlore and (B) $Mn_2Sb_2O_7$ structures. Filled corners of the isolated octahedra link to the adjacent HTB layer (not shown). Broken line is the projection of the trigonal unit cell.

trirutile (*18*) polymorphs with this composition.

The structure of γ-$MnSb_2O_6$ has been determined from X-ray powder diffraction data and shown to be related to, but distinct from, that of the tellurates and uranates with the Na_2SiF_6 structure. Both structures can be described as hexagonal close-packed oxygen arrays with cations occupying half the octahedrally coordinated sites. In both structures the same sites are occupied by cations, but the distribution of the different cations between the sites is different. This difference is readily explained by consideration of the cation radii. $MnSb_2O_6$ has the general formula AB_2X_6 while NiU_2O_6, CoU_2O_6, In_2TeO_6, Sc_2TeO_6, and Na_2SiF_6 have the general formula A_2BX_6 where A and B denote the larger and smaller cations, respectively.

In conclusion, this paper sounds a note of caution against describing compounds as pyrochlores on the basis of a general formula $A_2B_2O_7$, an approximately face-centered cubic subcell with lattice parameters of about 5 Å, and some supercell reflexions with positions corresponding to a doubling of the subcell parameters. There are numerous cation arrangements of the fluorite-related type which would satisfy these conditions, only one of which is the pyrochlore type. The critical test is that pyrochlore ordering of the cations must adequately explain the intensities, as well as the positions, of the X-ray reflexions. $Mn_2Sb_2O_7$ is a relatively recent example where this test is failed, but there are many other reported pyrochlores which might repay a similarly critical reexamination.

Appendix

If $Mn_2Sb_2O_7$ has a structure which is a small homogeneous distortion of the pyrochlore type, the relative intensities of the 101 and 003 reflexions should be 3 : 1, determined primarily by their multiplicities, since both these reflexions derive from 111_p reflexion (the subscript p denotes indices with reference to the pyrochlore axes: indices without subscripts refer to the hexagonal axial set). In fact the observed intensity ratio is 10 : 13. Similarly the 021, 113, 105 triplet derived from 311_p has observed intensities in the ratios 10 : 0 : 3 compared with multiplicities in the ratios 1 : 2 : 1. Also the 102 reflexion, the strongest "supercell" reflexion, is derived from the 200_p reflexion which is systematically absent for the pyrochlore structure. Finally the observed 103 reflexion is not permitted by rhombohedral symmetry.

References

1. M. A. Aia, R. W. Mooney, and C. W. W. Hoffman, *J. Electrochem. Soc.* **110** 1048 (1963).
2. F. Brisse, D. J. Stewart, V. Seidl, and O. Knop, *Canad. J. Chem.* **50,** 3648 (1972).
3. M. Baccaredda, *Gazz. Chim. Ital.* **66,** 539 (1936).
4. A. W. Sleight, *Inorg. Chem.* **7,** 1704 (1968).
5. M. A. Subramanian, A. Clearfield, A. M. Umarji, G. K. Shenoy, and G. V. Subba Rao, *J. Solid State Chem.* **52,** 124 (1984).
6. M. A. Subramanian, G. Aravamudan, and G. V. Subba Rao, *Prog. Solid State Chem.* **15,** 55 (1983).
7. F. Jona, G. Shirane, and P. Pepinsky, *Phys. Rev.* **98,** 903 (1955).
8. R. S. Roth, *J. Res. Nat. Bur. Stand.* **62,** 27 (1959).
9. E. C. Subbarao, *J. Amer. Ceram. Soc.* **44,** 92 (1961).
10. S. Kemmler-Sack and W. Rüdorff, *Z. Anorg. Allg. Chem.* **344,** 23 (1966).
11. H. Bernotat-Wulf and W. Hoffman, *Naturwissenschaften* **67,** 141 (1980).
12. H. Bernotat-Wulf and W. Hoffman, *Z. Kristallogr.* **158,** 101 (1982).
13. H. G. Scott, *J. Solid State Chem.* **43,** 131 (1982).
14. S. Kemmler-Sack, *Z. Anorg. Allg. Chem.* **358,** 226 (1968).
15. J. A. Malone, J. F. Dorrian, O. Muller, and R. E. Newnham, *J. Amer. Ceram. Soc.* **52,** 570 (1969).
16. A. Zalkin, J. D. Forrester, and D. H. Templeton, *Acta. Crystallogr.* **17,** 1408 (1964).

17. K. BRANDT, *Ark. Kemi, Mineral. Geol. 17A,* 1 (1943).

18. F. SALA AND F. TRIFIRO, *J. Catal.* **41,** 1 (1976).

19. H. J. ROSSELL AND H. G. SCOTT, *J. Solid State Chem.* **13,** 345 (1975).

20. "International Tables for X-ray Crystallography," Vol. IV, p. 71 (J. A. Ibers and W. C. Hamilton, Eds.), Kynoch Press, Birmingham (1974).

21. H. G. SCOTT, *Acta Crystallogr. Sect. A* **37,** 456 (1981).

22. M. J. REDMAN, W. P. BINNIE AND W. J. MALLIO, *J. Less-Common Metals* **23,** 313 (1971).

23. R. D. SHANNON, *Acta Crystallogr. Sect. A* **32,** 751 (1976).

24. B. DARRIET, M. RAT, J. GALY, AND P. HAGENMULLER, *Mater. Res. Bull.* **6,** 1305 (1971).

25. K. YAGI AND R. S. ROTH, *Acta Crystallogr. Sect. A* **34,** 765 (1978).